

Mass-driven vortex collisions in flat superfluidsAndrea Richaud^{1,2,*}, Giacomo Lamporesi³, Massimo Capone^{1,4} and Alessio Recati³¹*Scuola Internazionale Superiore di Studi Avanzati (SISSA), Via Bonomea 265, I-34136 Trieste, Italy*²*Departament de Física, Universitat Politècnica de Catalunya, Campus Nord B4-B5, E-08034 Barcelona, Spain*³*Pitaevskii BEC Center, CNR-INO and Dipartimento di Fisica, Università di Trento, I-38123 Trento, Italy*⁴*CNR-IOM Democritos, Via Bonomea 265, I-34136 Trieste, Italy*

(Received 1 September 2022; revised 9 March 2023; accepted 11 May 2023; published 26 May 2023)

Quantum vortices are often endowed with an effective inertial mass, due, for example, to massive particles in their cores. Such “massive vortices” display new phenomena beyond the standard picture of superfluid vortex dynamics, where mass is neglected. In this work, we demonstrate that massive vortices are allowed to collide, as opposed to their massless counterparts. We propose a scheme to generate controllable, repeatable, deterministic collisional events in pairs of quantum vortices. We demonstrate two mass-driven fundamental processes: (i) the annihilation of two counter-rotating vortices and (ii) the merging of two corotating vortices, thus pointing out new mechanisms supporting incompressible-to-compressible kinetic-energy conversion, as well as doubly quantized vortex stabilization in flat superfluids.

DOI: [10.1103/PhysRevA.107.053317](https://doi.org/10.1103/PhysRevA.107.053317)**I. INTRODUCTION**

Quantum vortices are topological excitations characterized by the quantized circulation of the velocity field. Their appearance in a rotating system represents the “smoking gun” of superfluidity, since they are the most direct consequence of the existence of a macroscopic wave function associated with the superfluid [1]. They are observed in contexts as diverse as liquid helium [2,3], ultracold gases [4–6], superconductors [7], and quantum fluids of lights in nonlinear optical systems [8]. Their existence has been also speculated in neutron matter [9,10]. The vortex motion is responsible for the onset of dissipative phenomena [7,11], while the unbinding of vortex-antivortex pairs constitutes the ultimate mechanism destroying the quasi-long-range coherence in a two-dimensional (2D) system [12,13].

Vortices are often pictured as funnel-like holes, where the superfluid density goes to zero and around which the quantum fluid exhibits a swirling flow. However, in many physical systems, vortex cores are not simply empty, but turn out to be filled by other particles, following different mechanisms. Such filling particles can be thermal atoms which coexist with the superfluid fraction [3,14], quasiparticle bound states [11], atoms deliberately introduced to better trace vortex trajectories [15,16], or atoms of a different quantum fluid [17–24]. Irrespective of their microscopic origin, atoms trapped within vortex cores have a deep influence on the vortex dynamics.

In two-dimensional (2D) systems, vortices can be seen for many purposes as point-like objects whose dynamics is described by an effective Lagrangian. The number q characterizing the quantized circulation is referred to as the “charge” of the vortex. If the core is empty, the dynamics does not

contain any inertial term, and the equations of motion are of first order and dominated by the so-called Magnus force. The presence of a dressed core, however, makes the vortex massive and calls for the inclusion of inertial terms.

The need for the inclusion of a mass term in the dynamics of vortex-like structures (skyrmions) was discussed in the context of magnets more than 30 years ago [25,26] (see Ref. [27] and references therein for a recent discussion). Although the physical origin of the mass can be rather different from what is discussed here, its effect on the skyrmion dynamics is the same. Around 10 years ago, an inertial term was discussed by Turner [28], studying polar-core vortices in the easy-plane phase of spin-1 condensates. A Lagrangian formulation and the comparison with numerical simulations of the full Gross–Pitaevskii equation (GPE) describing the gas can be found in Ref. [29]. Recently it was shown [20,21,30] that the inertial term in the particle-like description of vortices arises naturally in highly unbalanced Bose-Bose mixtures, where the majority component hosts a vortex, whose core is filled by the minority one. This provided a clear interpretation of the rise of the vortex mass as due to the dynamics of the minority component.

In this work, we show that, even in the absence of dissipation mechanisms ensuing, e.g., from the interaction with the thermal component, the presence of massive particles trapped within vortex cores opens the door to a new class of phenomena, when more than a single vortex is considered. While massless vortices can only interact at a distance, without getting too close one to each other [31,32], we find that massive vortices can actually collide and merge or annihilate, depending on their charge. We focus on two fundamental classes of two-vortex collisions: the collision of vortices with opposite or equal circulation. In the former case, the collision results in their mutual annihilation and in the consequent emission of sound waves. In the latter case, the collision of two singly quantized ($q_1 = q_2 = \pm 1$) vortices results in the formation of

*Corresponding author: andrea.richaud@upc.edu

a doubly quantized vortex $q = \pm 2$, a seemingly unstable state [33–36], which is instead stabilized by the presence of core mass, which, in turn, plays the role of an effective pinning potential [37]. We focus on the specific case of vortices in the majority component of a strongly unbalanced quasi-2D BEC mixture. We propose a realistic experimental protocol, where two-vortex collisions can be observed in a controlled fashion thanks to a component-selective potential.

II. THEORETICAL MODEL

We consider an atomic Bose-Bose mixture formed by N_a atoms of species a and N_b atoms of species b whose atomic masses are m_a and m_b , respectively. The mixture is strongly confined in the z direction by a harmonic potential characterized by an oscillator length d_z , such that the atomic motion along z is frozen. At zero temperature, the gas realizes a binary BEC, characterized by the order parameters ψ_a and ψ_b . Their dynamics obeys the coupled GPEs [38]

$$i\hbar \frac{\partial \psi_i}{\partial t} = \left(-\frac{\hbar^2 \nabla^2}{2m_i} + V_{\text{tr}}^i + \sum_{j=a,b} g_{ij} N_j |\psi_j|^2 \right) \psi_i, \quad i = a, b, \quad (1)$$

where the quasi-2D couplings $g_{ij} = \sqrt{2\pi} \hbar^2 a_{ij} / (m_{ij} d_z)$ are given by intra- and interspecies s -wave scattering lengths a_{ij} , and effective masses $m_{ij} = (m_i^{-1} + m_j^{-1})^{-1}$.

A particular topological solution of the coupled GPEs is a vortex in one component, whose core is filled by the other component, which has a trivial phase profile. When the system is SU(2) symmetric (or close), such solutions are named magnetic vortices since the total density is almost unaffected (see Ref. [19] and reference therein). As long as the forces applied to the two components do not significantly alter the composite object, its dynamics—as for the standard vortex in a superfluid—can be described in terms of a Lagrangian for a point-like particle. However, a remarkable feature appears due to the filled vortex core: the dynamics is massive, i.e., the time evolution of vortex coordinates $(x_j, y_j) =: \mathbf{r}_j$ is governed by second-order differential equations. The introduction of inertial effects in superfluid vortex dynamics or, in other words, the fact that vortices' velocities $\{\dot{\mathbf{r}}_j\}$ are independent of vortex positions $\{\mathbf{r}_j\}$, opened the door to new dynamical regimes [16,20,21]. In the context of magnetic skyrmions, it has already been possible to prove that it is indeed necessary to add an effective mass to the standard Thiele model [39], which is inherently noninertial, in order to capture the observed trajectories [40,41]. Interestingly, in the context of half-quantum vortices in a two-component BEC, approaching trajectories of vortex dipoles have been observed by solving the GPEs [42]. Since the authors used the standard point-like model in their analysis, they had to conclude by conjecturing on the possible presence of an inertial mass.

In the present work, we study the effect of the vortex mass on the vortex collisional dynamics. To ensure the vortex stability during their dynamics, we consider an immiscible mixture, corresponding to $g_{ab}^2 > g_{aa}g_{bb}$ (see discussion on vortex stability in the Appendix D). Moreover, we consider $N_b \ll N_a$, such that the vortex core is small enough and the use of an effective point-like particle description is justified.

While in the above-mentioned works the cores play a passive role, since they merely constitute a sort of “heavy burden” affecting the standard superfluid vortex dynamics, here we flip the perspective and use the massive cores to actively drive vortex collisions in a controlled fashion. These collisions may indeed happen in a many-massive-vortex system, but determining their precise location and timing is difficult and strictly dependent on the detailed initial state of the system. On top of this, the complexity of the dynamics, as well as the chaotic character of vortex trajectories, hinders the possibility to attempt any comparison between theory and experiments.

To circumvent these difficulties, we focus on the simplest possible systems where collisions are possible: a pair of vortices with the same or opposite charge. This choice allows us to perform a theoretical investigation of vortex collisions by using an experimentally accessible protocol based on a component-selective trapping potential. We consider that the mixture is confined in a box potential of radius R , and that the minority component feels also a harmonic potential $V_{\text{tr}}^b = m_b \omega_b^2 r^2 / 2$.

Following Ref. [21], one can derive the effective Euler-Lagrange equations of motion for two massive vortices subject to V_{tr}^b (see Appendix A):

$$M_j \ddot{\mathbf{r}}_j = k_j \rho_a \hat{z} \times \dot{\mathbf{r}}_j + \rho_a \frac{k_j}{2\pi} \left[k_i \frac{\mathbf{r}_j - \mathbf{r}_i}{|\mathbf{r}_j - \mathbf{r}_i|^2} + k_j \frac{\mathbf{r}_j}{R^2 - r_j^2} + k_i \frac{R^2 \mathbf{r}_i - r_i^2 \mathbf{r}_j}{R^4 - 2R^2 \mathbf{r}_i \mathbf{r}_j + r_i^2 r_j^2} \right] - M_j \omega_b^2 \mathbf{r}_j, \quad (2)$$

where $\rho_a = m_a n_a = m_a N_a / (\pi R^2)$ is the planar mass density of component- a atoms, $k_j = q_j \hbar / m_a$ ($q_j \in \mathbb{Z}$) is the strength of the j th vortex, while $M_j = N_b m_b / 2$ is the mass of component- b cores (we assume, without loss of generality, that the total mass $M_b = m_b N_b$ is equally subdivided between the two vortices). The two terms $\propto \rho_a$ are well known and describe the contribution of the Magnus force, the intervortex interaction and the presence of a hard-wall confining potential (resulting in an image vortex) [44]. The term $M_j \ddot{\mathbf{r}}_j$ represents the Newton-like acceleration term ensuing from the presence of massive cores [20,21], while the last term is due to their being subject to a harmonic confinement. The adoption of a (massive)-point-vortex model is justified for vortex cores much smaller than R . In our case, the characteristic size ℓ_v of massive vortices depends also on the number of core particles [20], but, for the considered values of N_b , it is of the order of the healing length $\xi_a = \hbar / \sqrt{2m_a g_{aa} n_a}$, which, in turn, is typically much smaller than R in standard atomic BECs.

III. POSSIBLE EXPERIMENTAL PLATFORM

As a possible platform to implement our protocol, we consider a heteronuclear mixture of ^{87}Rb and ^{41}K atoms, both in the internal state $|F, m_F\rangle = |1, +1\rangle$. The two gases can be condensed in the same trap and present a favorable window of magnetic fields where the interspecies scattering length can be smoothly tuned and three-body losses minimized [45]. In the following, rubidium and potassium represent component a and component b , respectively, and in all the numerical analysis, we use $a_{aa} = 99 a_0$, $a_{bb} = 65 a_0$, and $a_{ab} = 163 a_0$, with

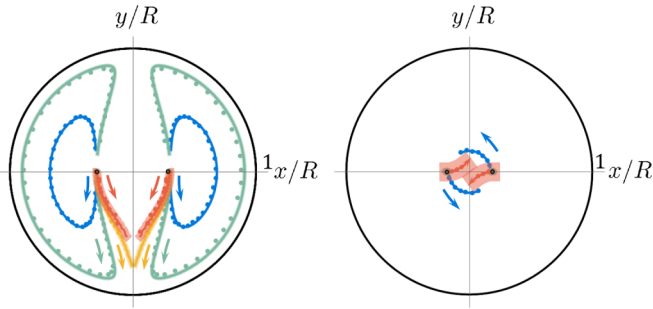


FIG. 1. Comparison between the massive point vortex model of Eq. (2) (solid lines) and GP simulations (dots). (left) Trajectories of two vortices with opposite sign, initially at a distance $d/R = 0.60$, for $N_b = 0, 1000, 3300$, and 5400 , respectively in blue, green, yellow and red. (right) Trajectories for two same-signed vortices, initially at a distance $d/R = 0.34$, for $N_b = 0$ and 13500 . The line thickness corresponds to the typical size of the filling BEC, ℓ_v . Other parameters used in the simulations for a mixture of ^{87}Rb and ^{41}K are $N_a = 5 \times 10^5$, $R = 25 \mu\text{m}$, $d_z = 0.82 \mu\text{m}$. $\omega_b = 85 \text{ rad/s}$ for the left panel, while $\omega_b = 250 \text{ rad/s}$ for the right panel. See related videos of GP simulations in the Supplemental Material [43].

a_0 being the Bohr radius. For the strong confining harmonic potential along z , we use $d_z = 0.82 \mu\text{m}$.

We consider two massive vortices that, at time $t = 0$, are symmetrically placed with respect to a diameter of the circular trap ($x_1 = -x_2$, $y_1 = y_2$) and are at rest. In the massless case, the motion of these vortices is well known and does not feature any collision: while the vortex dipole performs symmetric lobe-like orbits [11,31], the vortex pair exhibits a uniform circular orbit. These trajectories correspond to the light-colored lines in the left and right panels of Fig. 1. On the other hand, massive vortices subject to a species-selective confining potential feel an additional force able to catalyze the collision. Solving the equations of motion (2), one can notice (see dark lines in Fig. 1) that the intervortex distance $r_{12} := |\mathbf{r}_1 - \mathbf{r}_2|$ can tend to zero. For our purposes, we stopped the solution of Eqs. (2) at the time t_* such that $r_{12} = 2\ell_v$, at which the two quantum vortices are expected to undergo an actual collisional event. Solving the full GPEs with the same initial condition of Eq. (2), we find that the massive point vortex model gives very accurate results for $0 < t < t_*$ (dots and solid lines in Fig. 1 almost coincide).

IV. ANNIHILATION OF VORTEX-ANTIVORTEX PAIRS

In Fig. 2, we illustrate the GPE simulated dynamics of the density field ρ_a (upper row) and the phase field θ_a (lower row) associated with the condensate wave function $\psi_a = \sqrt{n_a}e^{i\theta_a}$ for the case of two counter-rotating vortices (the wave function associated with the minority component ψ_b is not shown because it is simply nonzero only within the vortex cores).

It is clear that, at $t = t_*$, the two quantum vortices collide and mutually annihilate. One can observe, in fact, that, for $t > t_*$, the density-depleted hole in ρ_a is associated with no phase singularities (the corresponding phase field θ_a is indeed trivial) and, for this reason, it should be only ascribed to the persistent presence of b particles which, being immiscible with respect to the a fluid, induce a local spatial phase sep-

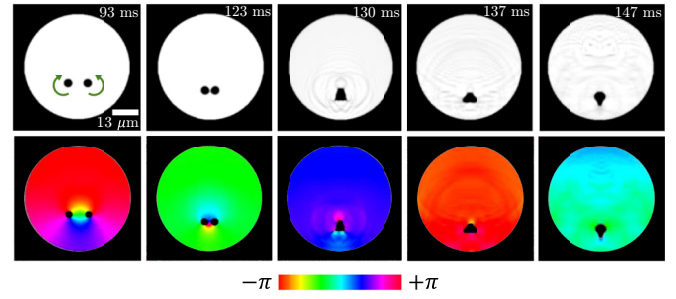


FIG. 2. Mass-driven collision of a pair of counter-rotating massive vortices. Starting from a pair of singly quantized vortices, upon colliding, the two vortices mutually annihilate and their incompressible kinetic energy is fully transferred into a sound pulse. First (second) row corresponds to the density (phase) field of the majority component (^{87}Rb). Here $N_b = 5400$ (the other microscopic parameters are listed in the caption of Fig. 1), the collision time t_* is 125 ms. See the full video of GP simulation in the Supplemental Material [43].

aration of the two components. On the other hand, a dramatic consequence of such annihilation process is the emission of an intense sound pulse, basically due to the conversion of vortex core and incompressible kinetic energies into phononic excitations [11,46]. This may have non-trivial implications in the context of quantum hydrodynamics [47] and quantum turbulence [48,49], as it constitutes an unexplored mechanism supporting the annihilation of single vortex-antivortex pairs.

V. MERGING OF SAME-SIGN VORTICES

The other fundamental class of two-vortex collisions involves two corotating vortices which, due to their tendency to repel each other, feature an intrinsic energy barrier that can be overcome thanks to the kinetic energy provided by the core mass. In Fig. 3, we illustrate the simulated GP dynamics, clearly showing the merging of two singly quantized vortices into a doubly quantized one. The latter state is known to be dynamically unstable [33–35] and prone to splitting in the massless case (see also Ref. [11] for a real-time observation),

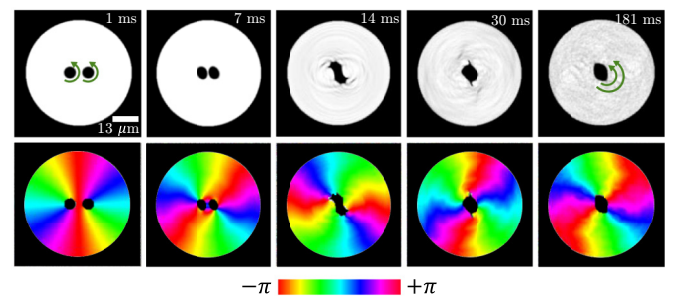


FIG. 3. Mass-driven collision of a pair of corotating massive vortices. Starting from a pair of singly quantized vortices, upon collision, a single doubly quantized vortex is stabilized. Same microscopic model parameters (except that $N_b = 1.35 \times 10^4$ and $\omega_b = 250 \text{ rad/s}$) and graphical conventions of Fig. 2. The collision time is $t_* = 9 \text{ ms}$. See the full video of GP simulation in the Supplemental Material [43].

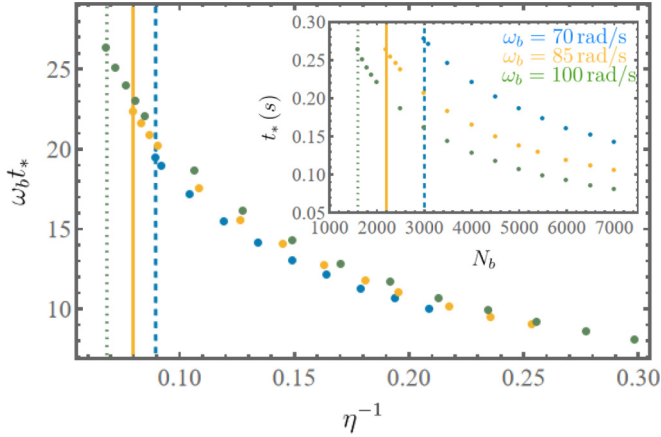


FIG. 4. Increasing the number of core atoms ($N_b \propto \eta^{-1}$), the vortices get heavier and the collisional time (t_*) decreases. Below a critical value of N_b (vertical lines), cores are too light and vortices do not collide at all. The stronger the harmonic confinement acting on component- b atoms, the smaller are the collision time and the critical value for N_b . The main panel illustrates the data upon a suitable nondimensionalization procedure mirroring the emergence of only one characteristic parameter η , while the inset shows the original data in dimensionful units. Same model parameters and initial conditions of Fig. 2 were used. The blue dashed, yellow solid, and green dotted lines correspond to 70, 85, and 100 rad/s, respectively. In the main panel (inset), from bottom to top (from top to bottom), data corresponding to 70, 85, and 100 rad/s are illustrated, respectively.

but it is stabilized by the presence of component- b particles. These particles, therefore, not only guide the collision of the two vortices as actively driving pinning centers, but also stabilize the resulting doubly quantized vortex (in view of an actual experimental realization, we argue that doubly quantized vortices should be robust with respect to weak-dissipation processes, since thermal atoms are expected to be repelled by the core-filling component). This result is far from being trivial and opens the door to the stabilization of multiply quantized vortices in BECs, even in the absence of an external pinning potential [37]. An external pinning potential would freeze the position of the vortex, while the presence of a massive core stabilizes the multiply quantized vortex without constraining its motion. Unexpectedly, also in this case, the collision of the two quantum vortices is inelastic, as it comes with the emission of sound waves. This represents an additional mechanism supporting the conversion of incompressible kinetic energy into compressible kinetic energy [50–53]. The dissipation of vortex energy underlies central problems in quantum hydrodynamics [47], such as the decay of quantum turbulence [54,55].

VI. COLLISION TIME

To further substantiate the discussed collisional events and their being robust with respect to variations of microscopic parameters, we computed the collision time t_* for different values of N_b and ω_b . As illustrated in Fig. 4, heavier core masses (larger values of N_b) correspond to faster collisions, i.e., to smaller values of t_* . The latter can be further lowered by increasing ω_b , the strength of the component- b trapping

potential, which we recall to be the catalyst of two-vortex collisions in the platform presented. Also, given a specific value of ω_b , there exist a critical number \tilde{N}_b of component- b atoms below which the two vortices are too light to collide (see vertical lines in Fig. 4). We further comment on the relation $\tilde{N}_b(\omega_b)$ (Appendix C), on the robustness of massive vortices (Appendix D), as well as on similar collisional protocols featuring larger initial vortex separations (Appendix B). Interestingly, the equations of motion for the vortex dipole can be shown to depend on a single effective model parameter $\eta := k\rho_a/(M\omega_b)$ and can be rewritten with respect to a new set of coordinates, the center of mass, and the relative displacement. This circumstance (see Appendix C) is illustrated in Fig. 4, where data associated with different values of ω_b and N_b are shown to collapse on the same curve upon suitable nondimensionalization.

VII. POSSIBLE EXPERIMENTAL IMPLEMENTATION

In the following, we propose a possible realistic experimental implementation for the observation of the merging and annihilation of massive vortices. A first requirement is immiscibility. This can be realized either using different species or different spin states. Depending on the kind of mixture, different methods and experimental techniques can be used. Besides being immiscible and stable (no spin relaxation or collisional decay channels), the mixture must allow for the possibility to handle it with component-selective potentials without excessive heating. As anticipated before, a mixture of ^{87}Rb and ^{41}K , both in the $|1, +1\rangle$ state, appears as a very promising candidate because the intraspecies scattering lengths are both positive and the interspecies one can be easily tuned around the Feshbach resonance at 78 G [45] to select the proper immiscibility condition. Furthermore it is stable versus spin relaxations, both species being in a stretched spin state. The wavelengths for the D_1 and D_2 transitions for K and Rb are $\lambda_{D_1, D_2}^{\text{K}} = 770$ nm, 766.5 nm and $\lambda_{D_1, D_2}^{\text{Rb}} = 795$ nm, 780 nm. In this way, it is convenient to use Rb as component a and selectively trap K with a focused Gaussian beam with a tune-in wavelength for Rb at 790 nm [56–58], both for the initial positioning of the minority b component and also for the species-selective harmonic confinement. The mixture can be initially trapped in a flat-box optical trap, realizable with DMD technology [59] and able to confine both components in a circular region. A repulsive optical barrier can be spun [11,31,60,61] around such large impurities clockwise or counterclockwise depending on the vortex charge which one wants to have in the majority component a . Alternatively, vorticity can be introduced through phase imprinting, by illuminating the atomic sample with a light pattern corresponding to the desired phase pattern [62]. In this case the regions where phase 0 and 2π connect should be depleted using a repulsive potential to avoid unwanted smooth phase profiles in the wrong direction [63]. Once vortices are created in component a , the pinning potential for component b can be removed while activating the harmonic potential to study the vortex dynamics. In the alternative case of using a spin mixture of a single atomic species, with a proper choice of magnetic states, one could also use a magnetic harmonic trap concentric with the optical box and prepare species a in a magnetic insensitive

state $m_F = 0$, while b in a low-field-seeker state. The density of the minority component can be directly imaged in the plane to observe the collision. Furthermore one can measure the vorticity in the majority component after the merging event, through Bragg interferometric measurements [64] or by removing the species-selective potential and observing the formation of singly quantized vortices.

VIII. CONCLUSIONS

In conclusion, we have shown that the inertial effect of particles deliberately or accidentally trapped in the cores of quantum vortices opens the door to two-vortex collisions, a scenario that has no counterpart within standard superfluid vortex dynamics [31,32], i.e., in systems where the dissipation ensuing from the interaction with the thermal component is negligible. We have presented a realistic experimental platform involving a quasi-2D imbalanced mixture of BECs which allows one to design and observe two-vortex collisions in a controlled fashion. The proposed protocol relies on the use of a component-selective potential [56–58], which catalyzes the occurrence of collisions in two-vortex systems. The massive cores do not simply alter standard vortices trajectories [21], but play the role of effective pinning potentials driving quantum vortices to collide. We demonstrate the mutual annihilation of vortex dipoles and the ensuing radiation of sound pulses, as well as the merging of two singly quantized vortices resulting in the stabilization of a doubly quantized vortex in the absence of an external pinning [37]. In addition, our results provide a clear explanation to previous numerical observations of half-quantum vortex collisions [42]. This interpretation will also be important to get a better insight about the superfluid turbulent behavior of such a system [65].

The studied phenomenology is expected to be rather general, as it originates only from the presence of trapped particles within—or equivalently a mass of—the quantum vortices, a circumstance which is quite common in many superfluid and magnetic systems. Possible future research directions include, but are not limited to, the study of the celebrated Berezinskii-Kosterlitz-Thouless transition [12] in the presence of a mechanism supporting the annihilation of (massive) vortex-antivortex pairs, the search for possible negative-temperature states [66,67], inverse energy cascade [68–70], a detailed analysis of the sound pulse emitted upon the collision, and its intriguing connections with gravitational phenomena, such as the collision of black holes [71]. Furthermore, this work could be extended from 2D to three dimensions (3D), including the contribution of Kelvin waves and reconnections [72,73].

ACKNOWLEDGMENTS

We thank C. Fort for providing useful data on the K-Rb mixture and P. Massignan for stimulating discussions. We acknowledge funding by Provincia Autonoma di Trento and from MIUR through the PRIN 2017 (Prot. 20172H2SC4 005), PRIN 2020 (Prot. 2020JLZ52N 002) programs and PNRR MUR Project No. PE0000023-NQSTI. A. Richaud received funding from the European Union’s Horizon research and innovation programme under the

Marie Skłodowska-Curie Grant Agreement *Vortexons* no. 101062887, by Grant No. PID2020-113565GB-C21 funded by MCIN/AEI/10.13039/501100011033, and by Grant No. 2021 SGR 01411 funded by Generalitat de Catalunya.

APPENDIX A: THE MASSIVE POINT VORTEX MODEL

In the Thomas-Fermi (TF) regime, vortices can be regarded as point-like defects, a circumstance which implies that the overall density $n_a(x, y)$ is essentially uniform within the considered hard-wall trap of radius R , except in a small region of radius $\approx \xi_a$ centered at the vortex position $\mathbf{r}_j = (x_j, y_j)$. On the other hand, the presence of a vortex of charge q_j in the atomic cloud has a profound impact on the phase field $\theta_a(x, y)$ of the condensate (we recall that $\psi_a = \sqrt{n_a}e^{i\theta_a}$). It is well known that, in the case of a circular potential well with hard walls, the velocity field $\mathbf{v} = \frac{\hbar}{m_a} \nabla \theta_a$ associated with the condensate- a wave function is such that its normal component must vanish at the boundary of the well [44]. This condition is ensured by the presence of image vortices of opposite circulation at the external positions $\mathbf{r}'_j = \mathbf{r}_j R^2 / r_j^2$.

A standard way to capture the dynamics of the field ψ_a in the presence of N_v vortical excitations is to develop a time-dependent variational approach [20,44,74]. One makes a time-dependent variational ansatz for the field $\psi_a = \sqrt{n_a}e^{i\theta_a}$, which, in our case, is given by

$$\theta_a(x, y) = \sum_{j=1}^{N_v} q_j \left[\arctan \left(\frac{y - y_j}{x - x_j} \right) - \arctan \left(\frac{y - y'_j}{x - x'_j} \right) \right], \quad (\text{A1})$$

and where the vortices coordinates $\mathbf{r}_j(t) = (x_j(t), y_j(t))$ are the only parameters assumed to depend on time. Then, one computes the Lagrangian functional

$$\mathcal{L}_a[\psi_a] = \mathcal{T}_a[\psi_a] - \Delta \mathcal{E}_a[\psi], \quad (\text{A2})$$

where

$$\mathcal{T}_a[\psi_a] = \int \frac{i\hbar}{2} \left(\psi_a^* \frac{\partial \psi_a}{\partial t} - \frac{\partial \psi_a^*}{\partial t} \psi_a \right) d^2r \quad (\text{A3})$$

is the kinetic term and

$$\Delta \mathcal{E}_a[\psi_a] = \int |\psi_a|^2 \frac{1}{2} m_a v_a^2 d^2r = \int n_a \frac{\hbar^2}{2m_a} (\nabla \theta_a)^2 d^2r \quad (\text{A4})$$

is the energy difference with respect to the vortex-free state. $\Delta \mathcal{E}_a$ is formally divergent in a vorticious flow, because the superfluid velocity behaves as $1/|\mathbf{r} - \mathbf{r}_j|$ around each vortex core. To regularize it, one customarily excludes a circular region of radius ξ_a around each vortex core.

One thus remains with an effective point-like Lagrangian which governs the dynamics of the assumed time-dependent variational parameters and thus provides an effective description of the system’s dynamics. The application of the time-dependent variational approach to a many-vortex system in a quasi-2D Bose-Einstein condensate is described in Ref. [44].

The presence of massive particles trapped within the vortices core modifies the “bare” vortex dynamics both because of their inherent inertial contribution [20,21] and because of the (radial) force $F = -\partial V_{\text{tr}}^b / \partial r = -m_b \omega_b^2 r$ which

component- b particles are subject to. Both effects can be incorporated into the (massless) point vortex model (A2). As in Refs. [21,74], for the localized b -component, we introduce the following time-dependent Gaussian ansatz:

$$\psi_b(\mathbf{r}) = \sum_{j=1}^{N_v} \sqrt{\frac{N_b}{\pi\sigma^2 N_v}} e^{-|r-r_j(t)|^2/2\sigma^2} e^{i\mathbf{r}\cdot\boldsymbol{\alpha}_j(t)}, \quad (\text{A5})$$

representing an array of N_v localized wave packets with width σ centered at $\mathbf{r}_j(t)$ and where the parameter $\boldsymbol{\alpha}_j(t)$ allows for a nonzero translational velocity $\dot{\mathbf{r}}_j = \hbar\boldsymbol{\alpha}_j/m_b$. In principle, the b -component core size σ depends on a number of microscopic parameters, including interaction constants (g_a, g_b, g_{ab}), the number of atoms in the two components (N_a, N_b), their atomic masses (m_a, m_b), the trap radius (R), and the condensate thickness (d_z) [20,75], but, for the point model to be valid, one only requires that $\sigma \ll R$.

A straightforward analysis based on the time-dependent variational approach reviewed above (see also Refs. [21,74]) leads to the effective point-like Lagrangian for species- b cores

$$\mathcal{L}_b = \sum_{j=1}^{N_v} \left[\frac{N_b m_b}{2N_v} \dot{\mathbf{r}}_j^2 - \frac{1}{2} \frac{N_b m_b}{N_v} \omega_b^2 r_j^2 \right], \quad (\text{A6})$$

which depends on both the average position \mathbf{r}_j and average velocity $\dot{\mathbf{r}}_j \propto \boldsymbol{\alpha}_j$ of each wave packet in Eq. (A5). Notice that this Lagrangian includes both the Newtonian inertial term $\propto \dot{\mathbf{r}}_j^2$ and the effect of the external confining potential $\propto r_j^2$.

As explained in Ref. [21], the effective dynamics of the overall composite system, i.e., of component- a vortices filled by component- b particles, can be described in terms of the following Lagrangian, here specialized to the case of $N_v = 2$ vortices

$$\begin{aligned} \mathcal{L}_{\text{tot}} &= \mathcal{L}_a + \mathcal{L}_b \\ &= \sum_{j=1}^2 \left[\frac{M_j}{2} \dot{\mathbf{r}}_j^2 + \frac{k_j \rho_a}{2} \dot{\mathbf{r}}_j \times \mathbf{r}_j \cdot \hat{\mathbf{z}} \right] - V(\mathbf{r}_1, \mathbf{r}_2), \end{aligned} \quad (\text{A7})$$

where

$$\begin{aligned} V &= \frac{\rho_a}{4\pi} \left\{ k_1 k_2 \ln \left(\frac{R^2 - 2\mathbf{r}_1 \cdot \mathbf{r}_2 + r_1^2 r_2^2 / R^2}{r_1^2 - 2\mathbf{r}_1 \cdot \mathbf{r}_2 + r_2^2} \right) \right. \\ &\quad \left. + k_1^2 \ln \left(1 - \frac{r_1^2}{R^2} \right) + k_2^2 \ln \left(1 - \frac{r_2^2}{R^2} \right) \right\} + \sum_{j=1}^2 \frac{1}{2} M_j \omega_b^2 r_j^2. \end{aligned} \quad (\text{A8})$$

APPENDIX B: COLLISIONS OF ARBITRARILY SPACED VORTICES

The collisional protocol illustrated in Figs. 1–3 is robust with respect to variations of the initial intervortex separation. In particular, within the proposed platform, it is possible to obtain vortex collisions also if the initial intervortex separation is larger than the distance between the vortex and the circular boundary (see Fig. 5). This is made possible by the presence of the harmonic potential which component- b atoms are subject to. As visible from the figure, in the case of counter-rotating vortices (left panel), for larger initial intervortex separations, the collision point is found closer to the circular boundary.

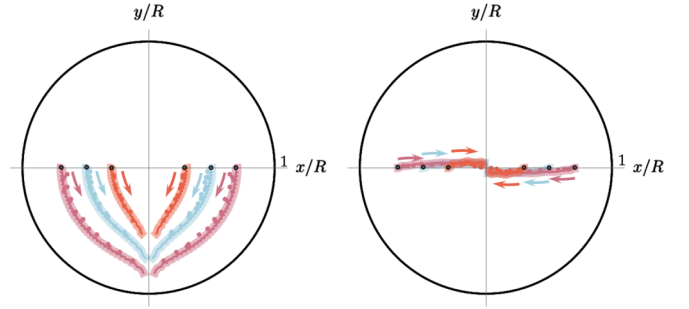


FIG. 5. The proposed collisional protocol is robust with respect to variations of the initial intervortex separation. Red, ice blue, and purple lines correspond to an initial distance of $0.6R$, R , and $1.4R$, respectively (black dots represent the starting positions). The left (right) panel corresponds to counter- (co-) rotating vortices. The assumed microscopic parameters are listed in the caption of Fig. 1. (left panel) $N_b = 5400$, $\omega_b = 85$ rad/s. (right panel) $N_b = 5000$, $\omega_{b,x} = 120$ rad/s, $\omega_{b,y} = 400$ rad/s for the red line, $\omega_{b,x} = 120$ rad/s, $\omega_{b,y} = 700$ rad/s for the ice-blue line, and $\omega_{b,x} = 80$ rad/s, $\omega_{b,y} = 700$ rad/s for the purple line. See related videos of GP simulations in the Supplemental Material [43].

On the other hand, the collisional protocol involving two corotating vortices requires a more careful design because of their repulsive interaction. Based on the point-like model (2), one may argue that collisions are always possible, provided that ω_b is large enough. Nevertheless, when performing GP simulations, one realizes that, if the harmonic force acting on the vortex cores exceeds a certain critical value, then component- b cores may be depinned from their hosting vortices. To circumvent this problem, it is enough to employ an anisotropic confining potential (namely $\omega_{b,x} \neq \omega_{b,y}$), which allows us to guide vortex collisions without triggering undesired adverse events such as the core depinning or the formation of additional vortices in the wake of the driven vortices. Adopting this trick, collisional protocols involving arbitrarily spaced vortices are possible, and the ensuing collision point is typically found at the trap's center (see right panel of Fig. 5 and related videos in the Supplemental Material [43]).

APPENDIX C: ANALYTICAL INSIGHT INTO THE ANNIHILATION OF A VORTEX DIPOLE

In the main text, we mentioned that the data illustrated in Fig. 4 collapse on the same curve upon suitable nondimensionalization. To better describe this peculiar property, let us rewrite motion equations (2) in dimensionless form. To this purpose, we choose ω_b^{-1} as timescale, and $\sqrt{M/m_a} \ell_b$ [where $\ell_b = \sqrt{\hbar/(M\omega_b)}$] as length scale. The resulting motion equations read

$$\begin{aligned} \ddot{\mathbf{r}}_j &= -\mathbf{r}_j + \eta \hat{\mathbf{z}} \times \dot{\mathbf{r}}_j + \eta \left[-\frac{\mathbf{r}_j - \mathbf{r}_i}{|\mathbf{r}_j - \mathbf{r}_i|^2} + \frac{\mathbf{r}_j}{R^2 - r_j^2} \right. \\ &\quad \left. - \frac{R^2 \mathbf{r}_i - r_i^2 \mathbf{r}_j}{R^4 - 2R^2 \mathbf{r}_i \cdot \mathbf{r}_j + r_i^2 r_j^2} \right], \end{aligned} \quad (\text{C1})$$

and manifestly features only one characteristic parameter $\eta := k\rho_a/(M\omega_b)$, as mentioned in the main text.

In the limit of large R , Eqs. (C1) can be written in terms of the center-of-mass $\mathbf{Q} = (\mathbf{r}_1 + \mathbf{r}_2)/2$ and relative $\mathbf{r} = \mathbf{r}_1 - \mathbf{r}_2$ coordinates as

$$\ddot{\mathbf{r}} = -\mathbf{r} + \eta \hat{z} \times 2\dot{\mathbf{Q}} - 2\eta \frac{\mathbf{r}}{r^2}, \quad (\text{C2})$$

$$\ddot{\mathbf{Q}} = -\mathbf{Q} + \frac{\eta}{2} \hat{z} \times \dot{\mathbf{r}}, \quad (\text{C3})$$

and therefore their solutions should depend only on the parameter η . With reference to Fig. 4, this explains the collapse of data obtained for different values of ω_b and N_b on the same curve. It is worth mentioning, as a technical caveat, that the various data points of Fig. 4 do not fall *exactly* on the same curve, but are slightly dispersed around it because the choice of using the same initial conditions [i.e., $x_1(0) = -x_2(0) = 0.3R$] when performing simulations in dimensionful units inevitably results in (slightly) different initial separations $|\mathbf{r}(0)|$ upon nondimensionalization. We have explicitly checked that, when initial conditions are chosen in such a way to be the same in dimensionless units, the collapse is perfect.

APPENDIX D: ROBUSTNESS OF MASSIVE VORTICES

According to the collisional protocol proposed in the main text, two vortices are led to collide by their massive cores, which thus play the role of actively driving pinning potentials. As a result, the trajectory $\mathbf{r}_j(t)$ of these vortices significantly differ from the one predicted by standard superfluid dynamics (compare the dark and light lines in Fig. 1). This implies that the massive core applies a non-negligible force on its hosting quantum vortex (and vice versa). If this force exceeds a certain critical value, the quantum-vortex–massive-core complex breaks down. More specifically, the massive core penetrates the vortex walls and enters the bulk of component- a condensate. The depinning of a massive core from its quantum vortex is a complex phenomenon, and its description requires a detailed analysis of the surface tension of component- a vortex walls, the compressibility properties of the majority component, as well as the miscibility of the two quantum fluids.

Although we are going to fully characterize this physics in a separate work, we anticipate that the discussed depinning occurs in regimes different from those presented in the main text. In essence, the rather-large (im)miscibility ratio $g_{ab}/\sqrt{g_a g_b} \approx 2.18$ characterizing our ^{87}Rb - ^{41}K mixture, together with the rather small values of the applied ω_b , ensure the robustness of our massive vortices, as well as the smooth running of the designed collisional protocol. We remark, in this regard, that smaller values of g_{ab} would lead to more fragile quantum-vortex–massive-core complexes, i.e., to structures which would be more prone to undergo depinning when subject to an acceleration. The acceleration $|\ddot{\mathbf{r}}_j(t)|$ experienced by massive vortices along their trajectories, from the very beginning of the collisional protocol to the collision itself, can be easily computed by means of Eq. (2). In Fig. 6, we illustrate the magnitude of this acceleration for the case of two counter-rotating massive vortices (we employ the same

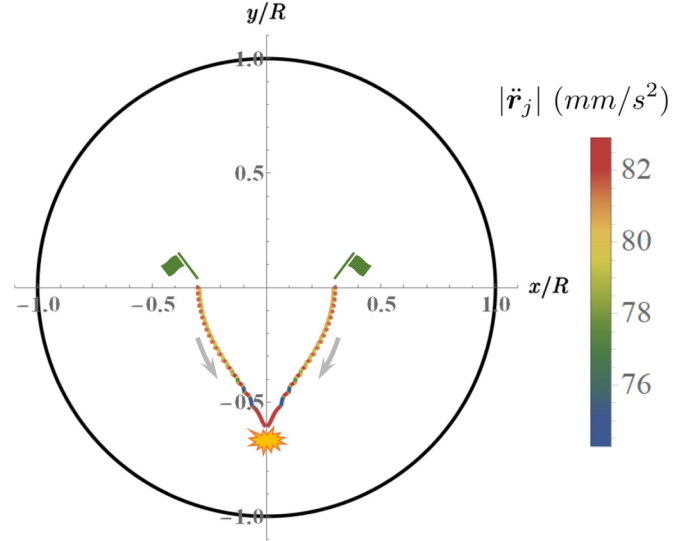


FIG. 6. The (magnitude of) the acceleration $|\ddot{\mathbf{r}}_j|$ of the two massive vortices along their collisional trajectories is maximum at the start (green flags), just before the collision (orange star) and at the changes of direction. Model parameters coincide with those used for Figs. 1–3.

model parameters used for the left panel of Fig. 1 and for Fig. 2).

The red color denotes those portions of trajectories where massive vortices are subject to the strongest stress, i.e., where the force exerted on the vortex walls by the massive core is maximum. Such portions correspond to the start of the dynamics, to the changes of direction (cusp-like features), and to the collision itself (orange star). They represent the segments where the depinning of a massive core from its

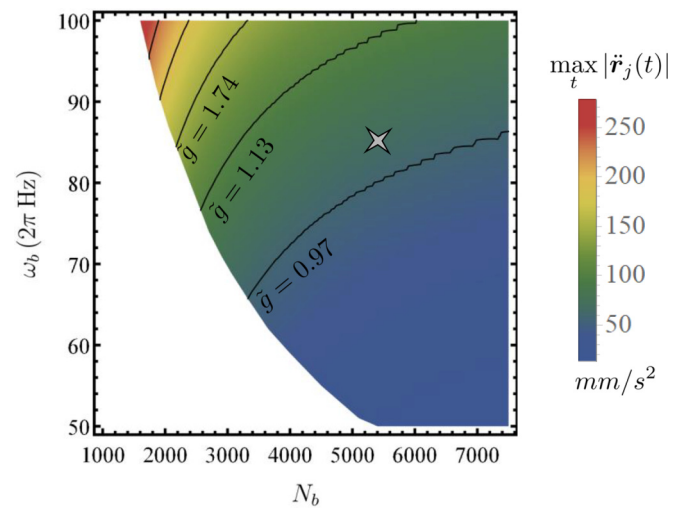


FIG. 7. Maximum acceleration experienced by a massive vortex before colliding [$\max_t |\ddot{\mathbf{r}}_j(t)|$] according to the collisional protocol illustrated in the left panel of Figs. 1 and 2. The same model parameters are assumed. The white region correspond to the absence of collisional events and its boundary represents the relation $\tilde{N}_b(\omega_b)$ mentioned in the main text.

quantum vortex may occur and their extent depends on the value of the component- b trapping frequency, ω_b . It is worth remarking, in this regard, that, if on the one hand, higher values of ω_b correspond to smaller collision times (t_*) (see Fig. 4), on the other hand, massive vortices would experience larger accelerations which could, in principle, break them before they come to collide. In Fig. 7, we plot the maximum acceleration experienced by a massive vortex before colliding, $\max_t \{|\ddot{\mathbf{r}}_j(t)|\}$.

Interestingly enough, each isoline can be associated with a critical value of $\tilde{g} := g_{ab}/\sqrt{g_a g_b}$ below which the massive core would undergo depinning before colliding. As visible in the figure, for the set of model parameters which we considered (gray cross), and given that the immiscibility ratio of our mixture is 2.18, our quantum-vortex–massive-core complexes are well within the stability region and hence can be safely subject to the accelerations needed to carry out the proposed collisional protocol without the risk of breaking.

-
- [1] L. Onsager, Statistical hydrodynamics, *Nuovo Cimento* **6**, 279 (1949).
 - [2] R. J. Donnelly, *Quantized Vortices in Helium II* (Cambridge University Press, Cambridge, 1991).
 - [3] M. M. Salomaa and G. E. Volovik, Quantized vortices in superfluid ^3He , *Rev. Mod. Phys.* **59**, 533 (1987).
 - [4] M. R. Matthews, B. P. Anderson, P. C. Haljan, D. S. Hall, C. E. Wieman, and E. A. Cornell, Vortices in a Bose-Einstein Condensate, *Phys. Rev. Lett.* **83**, 2498 (1999).
 - [5] K. W. Madison, F. Chevy, W. Wohlleben, and J. Dalibard, Vortex Formation in a Stirred Bose-Einstein Condensate, *Phys. Rev. Lett.* **84**, 806 (2000).
 - [6] M. W. Zwierlein, J. R. Abo-Shaeer, A. Schirotzek, C. H. Schunck, and W. Ketterle, Vortices and superfluidity in a strongly interacting Fermi gas, *Nature (London)* **435**, 1047 (2005).
 - [7] G. Blatter, M. V. Feigel'man, V. B. Geshkenbein, A. I. Larkin, and V. M. Vinokur, Vortices in high-temperature superconductors, *Rev. Mod. Phys.* **66**, 1125 (1994).
 - [8] I. Carusotto and C. Ciuti, Quantum fluids of light, *Rev. Mod. Phys.* **85**, 299 (2013).
 - [9] Ø. Elgarøy and F. V. D. Blasio, Superfluid vortices in neutron stars, *Astron. Astrophys.* **370**, 939 (2001).
 - [10] D. Peçak, N. Chamel, P. Magierski, and G. Wlazłowski, Properties of a quantum vortex in neutron matter at finite temperatures, *Phys. Rev. C* **104**, 055801 (2021).
 - [11] W. J. Kwon, G. Del Pace, K. Xhani, L. Galantucci, A. Muzi Falconi, M. Inguscio, F. Scazza, and G. Roati, Sound emission and annihilations in a programmable quantum vortex collider, *Nature (London)* **600**, 64 (2021).
 - [12] J. M. Kosterlitz, The critical properties of the two-dimensional xy model, *J. Phys. C: Solid State Phys.* **7**, 1046 (1974).
 - [13] Z. Hadzibabic, P. Krüger, M. Cheneau, B. Battelier, and J. Dalibard, Berezinskii–Kosterlitz–Thouless crossover in a trapped atomic gas, *Nature (London)* **441**, 1118 (2006).
 - [14] I. Coddington, P. C. Haljan, P. Engels, V. Schweikhard, S. Tung, and E. A. Cornell, Experimental studies of equilibrium vortex properties in a Bose-condensed gas, *Phys. Rev. A* **70**, 063607 (2004).
 - [15] G. P. Bewley, D. P. Lathrop, and K. R. Sreenivasan, Visualization of quantized vortices, *Nature (London)* **441**, 588 (2006).
 - [16] A. Griffin, V. Shukla, M.-E. Brachet, and S. Nazarenko, Magnus-force model for active particles trapped on superfluid vortices, *Phys. Rev. A* **101**, 053601 (2020).
 - [17] B. P. Anderson, P. C. Haljan, C. E. Wieman, and E. A. Cornell, Vortex Precession in Bose-Einstein Condensates: Observations with Filled and Empty Cores, *Phys. Rev. Lett.* **85**, 2857 (2000).
 - [18] K. J. H. Law, P. G. Kevrekidis, and L. S. Tuckerman, Stable Vortex–Bright-Soliton Structures in Two-Component Bose-Einstein Condensates, *Phys. Rev. Lett.* **105**, 160405 (2010).
 - [19] A. Gallemí, L. P. Pitaevskii, S. Stringari, and A. Recati, Magnetic defects in an imbalanced mixture of two Bose-Einstein condensates, *Phys. Rev. A* **97**, 063615 (2018).
 - [20] A. Richaud, V. Penna, R. Mayol, and M. Guilleumas, Vortices with massive cores in a binary mixture of Bose-Einstein condensates, *Phys. Rev. A* **101**, 013630 (2020).
 - [21] A. Richaud, V. Penna, and A. L. Fetter, Dynamics of massive point vortices in a binary mixture of Bose-Einstein condensates, *Phys. Rev. A* **103**, 023311 (2021).
 - [22] V. P. Ruban, Instabilities of a filled vortex in a two-component Bose–Einstein condensate, *JETP Lett.* **113**, 532 (2021).
 - [23] H. Zhu, D.-S. Wang, H. Yu, H.-Q. Cao, W.-M. Liu, and S.-G. Yin, Vortex-bright soliton complexes in $f=2$ rotating Bose–Einstein condensates, *Ann. Phys. (NY)* **437**, 168738 (2022).
 - [24] A. Chaika, A. Richaud, and A. Yakimenko, Making ghost vortices visible in two-component Bose-Einstein condensates, *Phys. Rev. Res.* **5**, 023109 (2023).
 - [25] B. Ivanov and V. Stephanovich, Two-dimensional soliton dynamics in ferromagnets, *Phys. Lett. A* **141**, 89 (1989).
 - [26] B. A. Ivanov and D. D. Sheka, Local magnon modes and the dynamics of a small-radius two-dimensional magnetic soliton in an easy-axis ferromagnet, *JETP Lett.* **82**, 436 (2005).
 - [27] X. Wu and O. Tchernyshyov, How a skyrmion can appear both massive and massless, *SciPost Phys.* **12**, 159 (2022).
 - [28] A. M. Turner, Mass of a Spin Vortex in a Bose-Einstein Condensate, *Phys. Rev. Lett.* **103**, 080603 (2009).
 - [29] L. A. Williamson and P. B. Blakie, Dynamics of polar-core spin vortices in a ferromagnetic spin-1 Bose-Einstein condensate, *Phys. Rev. A* **94**, 063615 (2016).
 - [30] A. Richaud, P. Massignan, V. Penna, and A. L. Fetter, Dynamics of a massive superfluid vortex in r^k confining potentials, *Phys. Rev. A* **106**, 063307 (2022).
 - [31] T. W. Neely, E. C. Samson, A. S. Bradley, M. J. Davis, and B. P. Anderson, Observation of Vortex Dipoles in an Oblate Bose-Einstein Condensate, *Phys. Rev. Lett.* **104**, 160401 (2010).
 - [32] S. W. Seo, B. Ko, J. H. Kim, and Y. Shin, Observation of vortex-antivortex pairing in decaying 2d turbulence of a superfluid gas, *Sci. Rep.* **7**, 4587 (2017).
 - [33] J. J. García-Ripoll and V. M. Pérez-García, Stability of vortices in inhomogeneous Bose condensates subject to rotation: A three-dimensional analysis, *Phys. Rev. A* **60**, 4864 (1999).

- [34] D. A. Butts and D. S. Rokhsar, Predicted signatures of rotating Bose–Einstein condensates, *Nature (London)* **397**, 327 (1999).
- [35] Y. Castin and R. Dum, Bose-Einstein condensates with vortices in rotating traps, *Eur. Phys. J. D* **7**, 399 (1999).
- [36] Y. Shin, M. Saba, M. Vengalattore, T. A. Pasquini, C. Sanner, A. E. Leanhardt, M. Prentiss, D. E. Pritchard, and W. Ketterle, Dynamical Instability of a Doubly Quantized Vortex in a Bose-Einstein Condensate, *Phys. Rev. Lett.* **93**, 160406 (2004).
- [37] T. P. Simula, S. M. M. Virtanen, and M. M. Salomaa, Stability of multi-quantum vortices in dilute Bose-Einstein condensates, *Phys. Rev. A* **65**, 033614 (2002).
- [38] Z. Hadzibabic and J. Dalibard, Two-dimensional Bose fluids: An atomic physics perspective, *Riv. Nuovo Cimento* **34**, 389 (2011).
- [39] A. A. Thiele, Steady-State Motion of Magnetic Domains, *Phys. Rev. Lett.* **30**, 230 (1973).
- [40] I. Makhfudz, B. Krüger, and O. Tchernyshyov, Inertia and Chiral Edge Modes of a Skyrmion Magnetic Bubble, *Phys. Rev. Lett.* **109**, 217201 (2012).
- [41] F. Büttner, C. Moutafis, M. Schneider, B. Krüger, C. M. Günther, J. Geilhufe, C. v. K. Schmising, J. Mohanty, B. Pfau, S. Schaffert, A. Bisig, M. Foerster, T. Schulz, C. A. F. Vaz, J. H. Franken, H. J. M. Swagten, M. Kläui, and S. Eisebitt, Dynamics and inertia of skyrmionic spin structures, *Nat. Phys.* **11**, 225 (2015).
- [42] K. Kasamatsu, M. Eto, and M. Nitta, Short-range intervortex interaction and interacting dynamics of half-quantized vortices in two-component Bose-Einstein condensates, *Phys. Rev. A* **93**, 013615 (2016).
- [43] See Supplemental Material at <http://link.aps.org/supplemental/10.1103/PhysRevA.107.053317> for videos illustrating Gross-Pitaevskii simulations of collisions of corotating and counter-rotating vortices.
- [44] J.-K. Kim and A. L. Fetter, Dynamics of a single ring of vortices in two-dimensional trapped Bose-Einstein condensates, *Phys. Rev. A* **70**, 043624 (2004).
- [45] A. Burchianti, C. D’Errico, S. Rosi, A. Simoni, M. Modugno, C. Fort, and F. Minardi, Dual-species Bose-Einstein condensate of ^{41}K and ^{87}Rb in a hybrid trap, *Phys. Rev. A* **98**, 063616 (2018).
- [46] M. Tylutki and G. Wlazłowski, Universal aspects of vortex reconnections across the BCS-BEC crossover, *Phys. Rev. A* **103**, L051302 (2021).
- [47] M. Tsubota, M. Kobayashi, and H. Takeuchi, Quantum hydrodynamics, *Phys. Rep.* **522**, 191 (2013).
- [48] C. F. Barenghi, L. Skrbek, and K. R. Sreenivasan, Introduction to quantum turbulence, *Proc. Natl. Acad. Sci. USA* **111**, 4647 (2014).
- [49] M. T. Reeves, K. Goddard-Lee, G. Gauthier, O. R. Stockdale, H. Salman, T. Edmonds, X. Yu, A. S. Bradley, M. Baker, H. Rubinsztein-Dunlop, M. J. Davis, and T. W. Neely, Turbulent Relaxation to Equilibrium in a Two-Dimensional Quantum Vortex Gas, *Phys. Rev. X* **12**, 011031 (2022).
- [50] A. S. Bradley and B. P. Anderson, Energy Spectra of Vortex Distributions in Two-Dimensional Quantum Turbulence, *Phys. Rev. X* **2**, 041001 (2012).
- [51] T. W. Neely, A. S. Bradley, E. C. Samson, S. J. Rooney, E. M. Wright, K. J. H. Law, R. Carretero-González, P. G. Kevrekidis, M. J. Davis, and B. P. Anderson, Characteristics of Two-Dimensional Quantum Turbulence in a Compressible Superfluid, *Phys. Rev. Lett.* **111**, 235301 (2013).
- [52] C. Nore, M. Abid, and M. E. Brachet, Kolmogorov Turbulence in Low-Temperature Superflows, *Phys. Rev. Lett.* **78**, 3896 (1997).
- [53] N. Navon, A. L. Gaunt, R. P. Smith, and Z. Hadzibabic, Emergence of a turbulent cascade in a quantum gas, *Nature (London)* **539**, 72 (2016).
- [54] A. W. Baggaley and C. F. Barenghi, Decay of homogeneous two-dimensional quantum turbulence, *Phys. Rev. A* **97**, 033601 (2018).
- [55] A. Lucas and P. Surówka, Sound-induced vortex interactions in a zero-temperature two-dimensional superfluid, *Phys. Rev. A* **90**, 053617 (2014).
- [56] J. Catani, G. Barontini, G. Lamporesi, F. Rabatti, G. Thalhammer, F. Minardi, S. Stringari, and M. Inguscio, Entropy Exchange in a Mixture of Ultracold Atoms, *Phys. Rev. Lett.* **103**, 140401 (2009).
- [57] G. Lamporesi, J. Catani, G. Barontini, Y. Nishida, M. Inguscio, and F. Minardi, Scattering in Mixed Dimensions with Ultracold Gases, *Phys. Rev. Lett.* **104**, 153202 (2010).
- [58] J. Catani, G. Lamporesi, D. Naik, M. Gring, M. Inguscio, F. Minardi, A. Kantian, and T. Giamarchi, Quantum dynamics of impurities in a one-dimensional Bose gas, *Phys. Rev. A* **85**, 023623 (2012).
- [59] N. Navon, R. P. Smith, and Z. Hadzibabic, Quantum gases in optical boxes, *Nat. Phys.* **17**, 1334 (2021).
- [60] K. C. Wright, R. B. Blakestad, C. J. Lobb, W. D. Phillips, and G. K. Campbell, Driving Phase Slips in a Superfluid Atom Circuit with a Rotating Weak Link, *Phys. Rev. Lett.* **110**, 025302 (2013).
- [61] E. C. Samson, K. E. Wilson, Z. L. Newman, and B. P. Anderson, Deterministic creation, pinning, and manipulation of quantized vortices in a Bose-Einstein condensate, *Phys. Rev. A* **93**, 023603 (2016).
- [62] G. Del Pace, K. Khani, A. Muzi Falconi, M. Fedrizzi, N. Grani, D. Hernandez Rajkov, M. Inguscio, F. Scazza, W. J. Kwon, and G. Roati, Imprinting Persistent Currents in Tunable Fermionic Rings, *Phys. Rev. X* **12**, 041037 (2022).
- [63] A. Kumar, R. Dubessy, T. Badr, C. De Rossi, M. de Goër de Herve, L. Longchambon, and H. Perrin, Producing superfluid circulation states using phase imprinting, *Phys. Rev. A* **97**, 043615 (2018).
- [64] S. Donadello, S. Serafini, M. Tylutki, L. P. Pitaevskii, F. Dalfovo, G. Lamporesi, and G. Ferrari, Observation of Solitonic Vortices in Bose-Einstein Condensates, *Phys. Rev. Lett.* **113**, 065302 (2014).
- [65] M. T. Wheeler, H. Salman, and M. O. Borgh, Relaxation dynamics of half-quantum vortices in a two-dimensional two-component Bose-Einstein condensate (a), *Europhys. Lett.* **135**, 30004 (2021).
- [66] G. Gauthier, M. T. Reeves, X. Yu, A. S. Bradley, M. A. Baker, T. A. Bell, H. Rubinsztein-Dunlop, M. J. Davis, and T. W. Neely, Giant vortex clusters in a two-dimensional quantum fluid, *Science* **364**, 1264 (2019).
- [67] S. P. Johnstone, A. J. Groszek, P. T. Starkey, C. J. Billington, T. P. Simula, and K. Helmersson, Evolution of large-scale flow from turbulence in a two-dimensional superfluid, *Science* **364**, 1267 (2019).
- [68] E. D. Siggia and H. Aref, Point-vortex simulation of the inverse energy cascade in two-dimensional turbulence, *Phys. Fluids* **24**, 171 (1981).

- [69] M. T. Reeves, T. P. Billam, B. P. Anderson, and A. S. Bradley, Inverse Energy Cascade in Forced Two-Dimensional Quantum Turbulence, *Phys. Rev. Lett.* **110**, 104501 (2013).
- [70] A. Skaugen and L. Angheluta, Origin of the inverse energy cascade in two-dimensional quantum turbulence, *Phys. Rev. E* **95**, 052144 (2017).
- [71] C. Barceló, S. Liberati, and M. Visser, Analogue gravity, *Living Rev. Relativ.* **14**, 1 (2011).
- [72] T. Simula, Vortex mass in a superfluid, *Phys. Rev. A* **97**, 023609 (2018).
- [73] S. Serafini, L. Galantucci, E. Iseni, T. Bienaimé, R. N. Bisset, C. F. Barenghi, F. Dalfovo, G. Lamporesi, and G. Ferrari, Vortex Reconnections and Rebounds in Trapped Atomic Bose-Einstein Condensates, *Phys. Rev. X* **7**, 021031 (2017).
- [74] V. M. Pérez-García, H. Michinel, J. I. Cirac, M. Lewenstein, and P. Zoller, Low Energy Excitations of a Bose-Einstein Condensate: A Time-Dependent Variational Analysis, *Phys. Rev. Lett.* **77**, 5320 (1996).
- [75] J. E. H. Braz and H. Tercas, Bound-state spectrum of an impurity in a quantum vortex, *Phys. Rev. A* **101**, 023607 (2020).